Electronic Materials Letters, Vol. 2, No. 1 (2006), pp. 49-52

Detection of the Rashba Effect in a Two-Dimensional Electron Gas

Jae Beom Ko, Hyun Cheol Koo*, Hyunjung Yi, Joonyeon Chang, and Suk Hee Han

Nano Device Research Center, Korea Institute of Science and Technology, Seoul 130-650, Korea

The Rashba effect induced by spin-orbit interaction is a key mechanism to realize spin transistors. The Rashba effect, which is necessary for spin control, is electrically detected by Shubnikov-de Haas oscillation (SdH) and potentiometric measurement. The node positions of the beat pattern from SdH oscillation make it possible to obtain 5.93 meV of spin splitting energy and 1.15×10^{-11} eV-m of Rashba constant in an inverted heterostruture at T = 1.8 K. A spin dependent chemical potential shift is also observed in an open circuit potentiometric geometry using ferromagnet electrode. Using a conventional HEMT (High Electron Mobility Transistor) structure, resistance change above 3 Ω is obtained for the potentiometric measurement at T = 5 K and 77 K.

Key words: Rashba effect, spin-orbit interaction, SdH oscillation, potentiometric measurement, HEMT structure

Spin field effect transistor (spin-FET) is strongly interested in the field of spin electronics because of high potential performance for high-speed switching and logic device. Several groups[1-4] have shown that the spin-polarized electrons are transferred in ferromagnet- semiconductor hybrid, all metal, and metal-insulator-metal systems. A spin-LED using ferromagnet and semiconductor heterostructure[5-6] has also been developed and spin polarization was detected successfully via an optical method. Considering broad device applications, devices with electrical detection such as spin-FET are more powerful. However, to date electrical spin detection efficiency is very low and spin transport with simultaneous gate modulation has yet to be realized.

The main concept of spin-FET[7] is that a spin orbit interaction in a semiconductor quantum well controls the spins of the injected carriers. In order to realize a spin-FET spin modulation by an electric field is necessary. Moving electrons (k_x) with a perpendicular electric field (E_z) induce an effective magnetic field (H_{Rashba}) to the y direction as shown in Fig. 1. This phenomenon is called the Rashba effect and the induced H_{Rashba} interacts with the magnetic moment of the electrons and controls the spin direction. Rashba Hamiltonian can be expressed as[1,7]

$$H_{SO}=\alpha(\boldsymbol{\sigma}\times\mathbf{k})\cdot\hat{\mathbf{z}}, \tag{1}$$

where α is the Rashba constant and σ are the Pauli matrices.

Even with a zero bias field, an interfacial electric field arising from asymmetry of the potential well of a two dimensional electron gas (2-DEG) system produces a Rashba term. At zero bias, the number of electrons with $k_x > 0$ is the same as that with $k_x < 0$. However for one specific k_x, spin subband asymmetry occurs and the value of spin splitting energy is proportional to $\mu_B H_{\mathrm{Rashba}}$. Note that μ_B is Bohr magnetron. The spin splitting energy between spin-up and -down can be expressed as[8]

$$\Delta_{SO}=2\alpha k_F, \tag{2}$$

where k_F is the Fermi wave number and α is the Rashba constant. Note that k_F is a function of carrier concentration. The Rashba effect causes the spin-up and -down subbands of the 2-DEG to have different conductances. A ferromagnetic electrode with parallel or antiparallel orientation of induced magnetic field can measure the spin dependent voltage shifts[9]. In this paper, we show two detection methods for the Rashba effect and numerical values that confirm the spin controllability in a HEMT (High Electron Mobility Transistor) system.

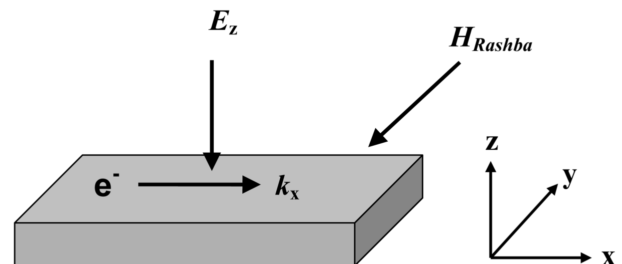

Fig. 1. Schematic explanation of the Rashba effect.

*Corresponding author: hckoo@kist.re.kr

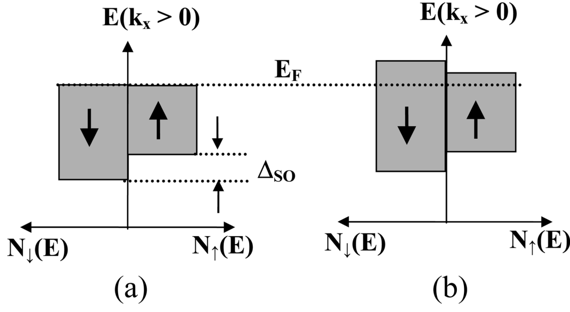

Fig. 2. Density of state in 2DEG for $k_x > 0$ (a) I = 0, (b) I = +I_x.

Figure 2(a) shows the density of state in 2DEG for $k_x > 0$ when the bias current is zero[9]. There are more spin-down carriers than spin-up carriers. For $k_x < 0$, similarly, the number of spin-up carriers is larger. The spin splitting energy Δ_{SO} is indicated in the diagram. If the current flows into the x direction, for $k_x > 0$ the Fermi levels of the spin-up and -down are unbalanced as shown in Fig. 2(b)[2,9]. The chemical potentials of both spin-up and -down become higher, but the chemical potential of the spin-down increases more than the spin-up chemical potential. Therefore, the Fermi level of the spin-down is higher than that of the spin-up. If the current is reversed, the chemical potential of the spin-down decreases more than the spin-up chemical potential and the Fermi level of spin-up becomes higher. In the same sense, the opposite phenomenon occurs when $k_x < 0$.

Figure 3(a) shows the schematic measurement set-up of Shubnikov-de Haas (SdH) oscillation. In order to define a 15 μm wide 2DEG mesa, ion milling was performed. Fig. 3(b) explains the origin of SdH oscillation[10]. The filled orbital is expressed as the shaded region. Electron transfer to a lower Landau level can occur because degeneracy increases as the magnetic field (B) is raised. For $B = B_1$ total energy shows maximum at Fermi level, but for $B = B_2$ total energy level is minimum. As increasing the magnetic field further, the maximum or minimum energy exists alternatively. This phenomenon is called the De Haas-van Alphen Effect, and SdH oscillation is a modified version for the resistance-field relationship. In other words, the lowest or the highest resistance corresponds to the maximum or the minimum energy, respectively, for SdH oscillation. Fig. 3(c) shows the energy diagram of the inverted heterostructure which is used for SdH oscillation measurement. In this structure the carrier supply layer is located below the active layer[8,11]. The doping concentration of the carrier supply layer is $7 \times 10^{18}/\mathrm{cm}^3$. $In_{0.52}Al_{0.48}As$ and $In_{0.53}Ga_{0.47}As$ cladding layers are potential barriers to confine the electrons inside the InAs channel. The thickness of the InAs active layer is only 2 nm so as to reduce the stress between the active layer and the InP substrate. The thickness of the upper $In_{0.52}Al_{0.48}As/In_{0.53}Ga_{0.47}As$ cladding layer is 20 nm/13.5 nm and that of the lower

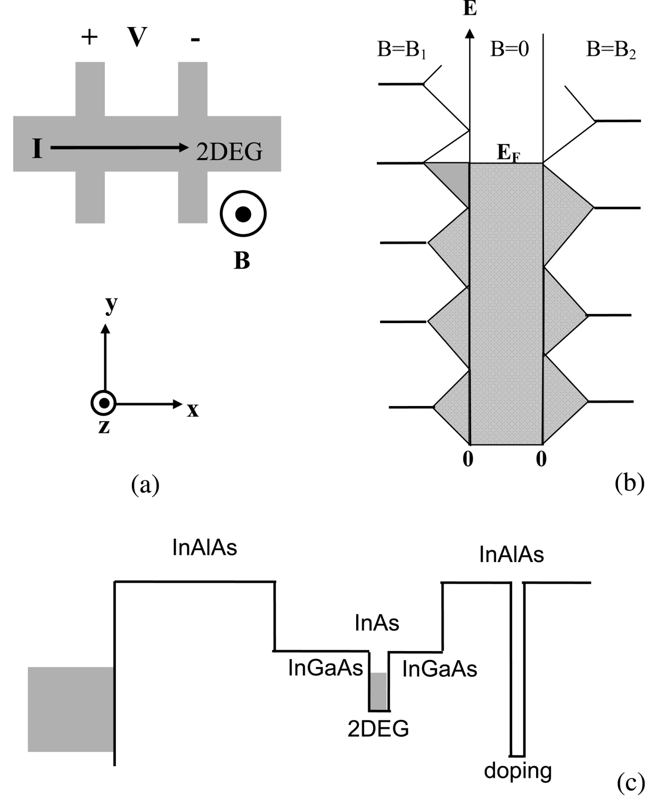

Fig. 3. (a) Measurement geometry for Shubnikov-de Haas oscillation. (b) Explanation of Shubnikov-de Haas oscillation. (c) Energy diagram of heterostructure.

$In_{0.53}Ga_{0.47}As/In_{0.52}Al_{0.48}As$ cladding layer is 2.5 nm/6 nm. In this HEMT structure, the quantum well is asymmetric due to the carrier supplier location and the different thickness of the cladding layers, and hence an interfacial electric field can arise even without an external electric field. The carrier concentration and the mobility of this InAs 2DEG at 300 K (16 K) are $6.34 \times 10^{12}/\mathrm{cm}^2$ ($4.60 \times 10^{12}/\mathrm{cm}^2$) and 5700 cm^2/V-s (34729 cm^2/V-s), respectively.

The measurement data of SdH oscillation using the same geometry as than in Fig. 3(a) is shown in Fig. 4. Major and minor spins have their own frequencies ($f_{\uparrow(\downarrow)}$), which depend on the carrier concentration ($n_{\uparrow(\downarrow)}$) as shown in Eq. (3)[12-14]:

$$f_{\downarrow(\uparrow)} = hn_{\downarrow(\uparrow)}/e. \tag{3}$$

When the two different frequency signals are combined, the beat patterns generate as shown in Fig. 4. Spin splitting energy can be expressed as[12-14]

$$\Delta_{SO} = 2\pi\eta^2 (n_\uparrow - n_\downarrow)/m^*. \tag{4}$$

As shown in Fig. 4, the nodes of the beat pattern are observed at B = 0.88 T and 1.34 T at T = 1.8 K. Using Eqs.(2)-(4) and the node positions, we obtain spin splitting energy (Δ_{so}) of 5.93 meV and of Rashba constant (α) of

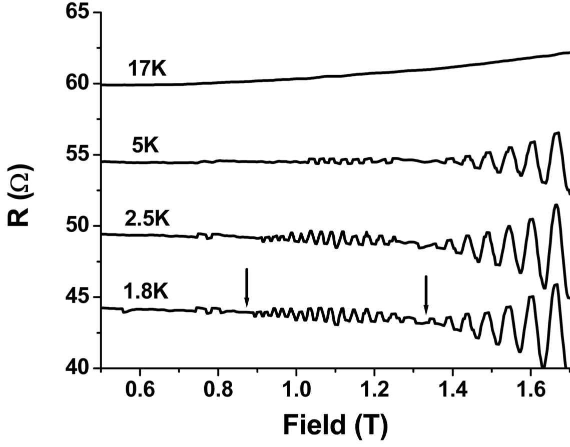

Fig. 4. Measurement data of Shubnikov-de Haas oscillation.

1.15×10^{-11} eV-m for this inverted heterosturcture. The beat patterns exist up to 5 K, but node positions are unclear with increasing temperature. This is attributed to the decrease of the spin orbit interaction with increasing temperature. Since the discrete energy level broadens at higher temperature, the oscillation disappears at T=17 K.

Figure 5(a) shows the measurement geometry for the potentiometric method in which the current was applied through the 2DEG and the voltage difference between the ferromagnet and the 2DEG was measured. In this measurement, an InAs channel quantum well structure[2,15] is used. The energy diagram of this heterostructure is shown in Fig. 5(b). A 30 Å top InAs layer acts as a capping layer preventing the $Al_{0.6}Ga_{0.4}Sb$ layer from oxidizing and reducing leakage current. A carrier supply layer is located at the center of the upper $Al_{0.6}Ga_{0.4}Sb$ layer and the doping concentration is 4×10^{18}/cm^3. A 15 nm-InAs 2DEG is formed between the two $Al_{0.6}Ga_{0.4}Sb$ layers. The 20 nm-upper $Al_{0.6}Ga_{0.4}Sb$ layer also acts as a low transmission layer, enhancing spin injection efficiency. Due to the structure asymmetry, an intrinsic electric field also arises in this structure. The carrier concentration and the mobility of this InAs 2DEG at 300 K (15 K) are 1.53×10^{11} /cm^2 (7.37×10^{11} /cm^2) and 19430 cm^2/V-s (66670 cm^2/V-s) respectively. The lateral dimensions of the ferromagnet ($Co_{0.9}Fe_{0.1}$) is 17 μm by 2.4 μm and the thickness is 60 nm.

The measured resistance value (R=V/I) in the potentiometric geometry of the sample with 800 nm wide and 150 nm long channels at 5 K are presented in Fig. 6(a). In order to prevent burnt-out due to the electrostatic force and resistive heating, seven channels are connected in parallel[16]. In Fig. 6(a) the ferromagnet (FM) appears to be saturated near 200 Oe in the field sweep up and down directions. The potential loop is slightly shifted to the left, and this shift may be due to the asymmetry or complexity of induced anisotropy during the deposition of the ferromagnetic electrode.

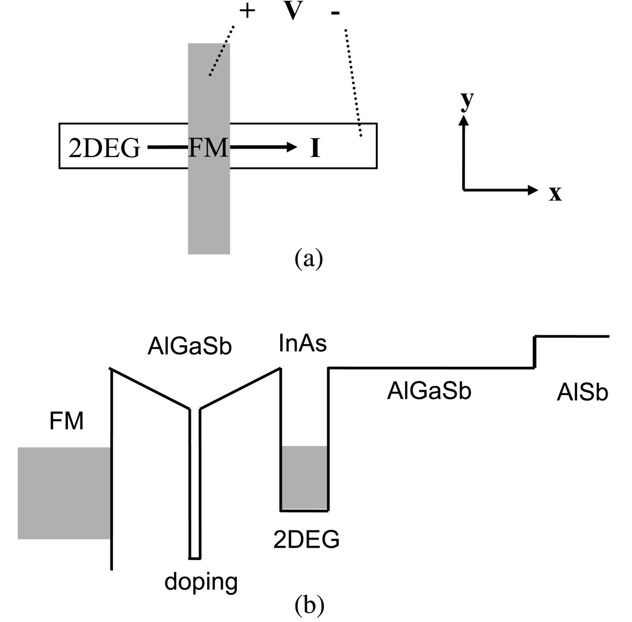

Fig. 5. (a) Measurement geometry for potentiometric measurement (b) Energy diagram of heterosturucture.

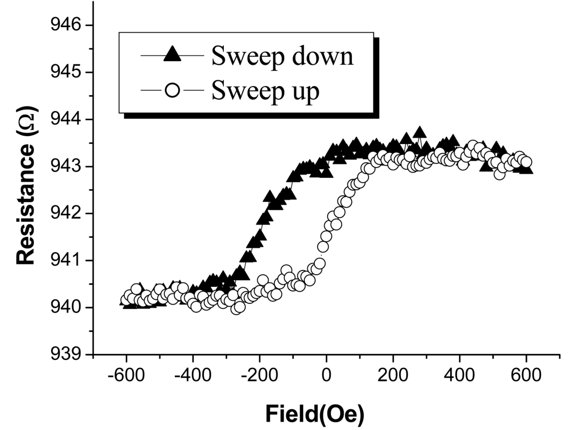

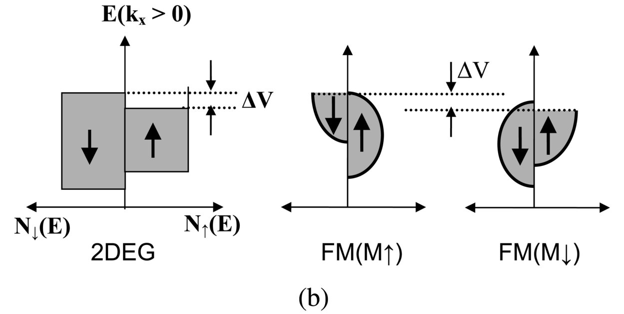

Fig. 6. (a) Results of potentiometric geometry. (b) Density of states and chemical potential shifts in potentiometric geometry.

Up to 77 K, a similar signal was detected; however the base line showed greater fluctuation. The potential difference ΔR

at 5 K is about 3.4 Ω and this value is nearly unchanged at 77 K. The mechanism of potentiometric geometry is the spin sub-band difference of up and down chemical potentials in the 2-DEG by changing the magnetization direction of the FM. This measurement gives a hysteresis loop-like potential curve. The origin of spin splitting is as follows. Spin-orbit coupling of the FM/2-DEG junction can arise from structure asymmetry in the confining quantum well. This asymmetry generates an electric field normal to the 2-DEG plane (E_z). The high mobility electrons traveling in the x direction in the 2-DEG experience the electric field (E_z) resulting in an effective magnetic field (H_y). This magnetic field shifts the sub-bands of up and down spins in the 2-DEG generating in a net magnetization in the 2-DEG whose orientation depends on the direction of the bias current. If the current direction is selected, the major spin can be also determined as shown in Fig. 6(b). The chemical potential of the FM is aligned with that of the 2-DEG. When the magnetization of the FM is the spin-up status, the chemical potential of the FM is aligned with the spin-down potential of the 2-DEG and the voltage probe displays a high value. If the FM magnetization is reversed, the chemical potential of FM is aligned with the spin-up potential of the 2DEG and the voltage probe displays a low value. The indicated ΔV is the same as the potential difference (I × ΔR) in Fig. 6(a). While this value, ΔV, is not the same as the spin splitting energy (Δ_{so}), it dose verify the existence of Rashba effect in this 2DEG structure,

In summary, we utilized two methods, SdH oscillation and potentiometric measurement, to detect the Rashba effect. In the results of SdH oscillation, the node positions of the beat pattern show 5.93 meV spin splitting energy and 1.15×10^{-11} eV-m Rashba constant in an InAs channel inverted heterostructure at T = 1.8 K. In potetiometric geometry, a spin dependent chemical potential shift is detected with a ferromagnet electrode. Using a conventional HEMT structure, a resistance change of 3.4 Ω is obtained at T = 5 K and 77 K. Spin splitting without an external magnetic field is an important factor to control the spin direction, and thus a channel with a large Rashba effect should be used for a spin-FET. Furthermore, in order to develop a spin FET, gate voltage controlled spin modulation and high spin injection efficiency are required.

ACKNOWLEDGMENT

This work was supported by the VISION 21 PROGRAM of KIST.

REFERENCES

1. P. R. Hammar and M. Johnson, *Phys Rev Lett.* **88**, 066806 (2002).
2. P. R. Hammar and M. Johnson, *Appl Phys Lett.* **79**, 2591 (2001).
3. F. J. Jedema, A. T. Filip, and B. J. van Wees, *Nature.* **410**, 345 (2001).
4. F. J. Jedema, H. B. Heersche, A. T. Filip, J. J. A. Baselmans, and B. J. van Wees, *Nature.* **416**, 713 (2003).
5. O. M. J. van't Erve, G. Kioseoglou, A. T. Hanbicki, C. H. Li, B. T. Jonker, R. Mallory, M. Yasar, and A. Petrou, *Appl. Phys. Lett*. **84**, 4334 (2004).
6. A. T. Hanbicki, O. M. J. van't Erve, R. Magno, G. Kioseoglou, C. H. Li, B. T. Jonker, G. Itskos, R. Mallory, M. Yasar, and A. Petrou, *Appl. Phys. Lett*. **82**, 4092 (2003).
7. S. Datta and B. Das, *Appl. Phys. Lett*. **56**, 665 (1990).
8. J. Nitta, T. Akazaki, and H. Takayanagi, *Phys. Rev. Lett*. **78**, 1335 (1997).
9. P. R. Hammar and M. Johnson, *Phys Rev B* **61**, 7207 (2000).
10. C. Kittel, *Introduction to Solid State Physics 7th ed.* p.257-260, John Wiley & Sons, Inc. (1996).
11. J. Nitta, T. Akazaki, H. Takayanagi, and Takatomo Enoki, *Physica E*. **2**, 527(1998).
12. Ikai Lo, J. K. Tsai, W. J. Yao, P. C. Ho, Li-Wei Tu, T. C. Chang, S. Elhamri, W. C. Mitchel, K. Y. Hsieh, J. H. Huang, H. L. Huang, and Wen-Chung Tsai, *Phys. Rev. B* **65**, 161306(R) (2002).
13. B. Das, D. C. Miller, S. Datta, R. Reifenberger, W. P. Hong, P. K. Bhattacharya, J. Singh, and M. Jaffe, *Phys. Rev. B* **39**, 1411 (1989).
14. J. Luo, H. Munekata, F. F. Fang, and P. J. Stiles, *Rev. B* **38**, 10142 (1989).
15. P. R. Hammar, B. R. Bennett, M. J. Yang, and M. Johnson, *J. Appl. Phys*. **87**, 4665 (2000).
16. Hyunjung Yi, H. C. Koo, W. Y. Kim, Joonyeon Chang, S. H. Han, and S. H. Lim, *J. Appl. Phys*. **97**, 10D502 (2005).